ELSEVIER

Ceramics International 26 (2000) 197–202

CERAMICS INTERNATIONAL

As-fired strength of sintered silicon nitride ceramics

Wenjea J. Tseng [a,*,1], Hideki Kita [b]

[a] Department of Materials Science and Engineering, I-Shou University, Ta-Hsu Hsiang, Kaohsiung, Taiwan 84008
[b] Isuzu Ceramics Research Institute, 8 Tsuchidana, Fujisawa-shi, Kanagawa-ken, 252 Japan

Received 9 November 1998; received in revised form 26 November 1998; accepted 22 February 1999

Abstract

An increased machined, bulk strength is seen to lead to an improved as-fired strength. Silicon nitride with an as-fired strength as high as 750 MPa can be obtained, sufficient for most structural applications. Microstructural examinations reveal that the reduction of surface and subsurface pores (or equivalent, may be treated as cracks) both in size and occurrence frequency is the primary reason for the strength increase observed. A linear elastic fracture mechanics model correlates the as-fired and bulk strength properties, and predicts that subsurface flaws located in a reasonably deep site underneath the surface would dominate the flexural strength if their length exceeds 2.3–2.8 times of the length of surface defects. The subsurface flaws very close to the surface are the most damaging and should be avoided by process optimizations.

Keywords: C. Fracture; D. Silicon nitride; As-fired strength; Defect size density

1. Introduction

Silicon nitride ceramics has long been recognized as candidate materials for many structural applications [1]. Steady improvements on its strength and reliability, as well as on its thermal properties for specific applications, have progressed the material to a new stage that recurrent interests on utilization of silicon nitride to various emerging applications gradually mature. However, the relatively high cost of ceramic components compared to metallic counterparts remains as a surmounting obstacle for a wider acceptance [2,3]. Therefore, improving the as-fired strength of sintered silicon nitride has attracted much industrial interest in recent years mainly because this approach is one of the alternatives for achieving cost-effective manufacturing.

In the literature, little has been devoted to this subject; therefore, a fundamental understanding specifically focused on failures of using the as-fired surface as a load-bearing medium is not well understood. A reliable method for improving the as-fired properties has consequently not been fully established. Until now, surface flaws as well as near-surface defects, especially the residual pores either located on or beneath the free surface, have been reported to be detrimental to the as-fired properties [4,5]. A residual, compressive stress on the sintered surface of ceramics was reported to result in an increase in the as-fired strength [6]. Surface strengthening may also be attained by formation of a surface coating onto the sintered ceramic substrates having existing defects on the free surface [7]. Nevertheless, a theoretical examination on strength-determining mechanisms is lacking and is inherently necessary in order to pave ways for further strengthening in a reproducible manner. In this study, we fractured various silicon nitride ceramics by placing the as-fired or machined surfaces under a bending tension and related these properties to a linear elastic fracture mechanics model, assuming that the catastrophic failure resulted from competing flaw populations residing on or beneath the free surface. Based on the strength comparison obtained, we aimed at, at least as a first step, bringing forward a tangible measure from both experimental and theoretical viewpoints for achieving a reproducible enhancement on the as-fired properties.

2. Materials and experimental procedures

Three types of silicon nitride ceramics were tested in this study. The materials denoted as SN-A and SN-B were both commercially available silicon nitride ceramics

* Corresponding author
[1] New address: Institute of Materials Science & Manufacturing, Chinese Culture University, Yang Min Shan, Taipei, Taiwan 11114.

0272-8842/00/$20.00
PII: S0272-8842(99)00040-1

(Kyocera's SN237 and SN235, respectively). Their fabrication processes are unknown. The third type of sintered material (referred to as SN-C) was prepared by a low gas pressure sintering and the fabrication details were described elsewhere [5]. Major sintering additives included yttria and alumina, and some trace amount of silica. All specimens presented a density exceeding 99% of the theoretical.

Bending specimens with a dimension of $3 \times 4 \times 45$ mm were prepared and their flexural strengths were determined by the four-point bend test with an inner and outer span of 10 and 30 mm, respectively. The flexural test was conducted by placing either the as-fired or machined surface on the bending tension side. For the machined specimens, down to 3 μm diamond polishing in the longitudinal direction of the parallelepiped samples was conducted prior to the fracture test and the removed thickness was about 500 μm from the free surface. Cross-head speed of the Instron machine (Model 1361, U.S.A.) was held constant during testing and was controlled at a speed of 0.5 mm per minute. About 10 to over 30 samples were fractured for each type of the specimens. Microstructure of fractographic and cross-sectional views were examined by both optical and scanning electron microscopy.

3. Results and discussion

3.1. Surface microstructure

The materials tested all exhibit a similar microstructure with self-reinforcing, abnormally-grown β-Si_3N_4 grains randomly embedded in a more equiaxed matrix forming an interlocking structure. The SN-A and B presented a virtually identical fractographic microstructure, as shown representatively in Fig. 1. For the SN-C material, a comparatively increased fraction of the abnormally grown β-Si_3N_4 grains both in size and quantity perspectives was observed (Fig. 2). The difference in grain size distribution of these silicon nitride specimens may have resulted from the original powder characteristics (e.g. α phase content, particle size, etc.) and variations in processing conditions. These large β-Si_3N_4 grains in the SN-C might hence become a fracture-initiating site, which in turn, would result in a reduced overall strength as will be described in the latter section.

The as-fired surface of the SN-A material is surprisingly smooth (Fig. 3), contrary to the SN-B and SN-C where protruding silicon nitride grains are apparent on the surface [5]. Examination of the cross-section of the SN-A material confirmed the surface smoothness [the maximum (peak-to-valley) surface roughness was less than about 3 μm] and revealed that only minor residual pores with a size ranging from 4 to 10 μm were observed

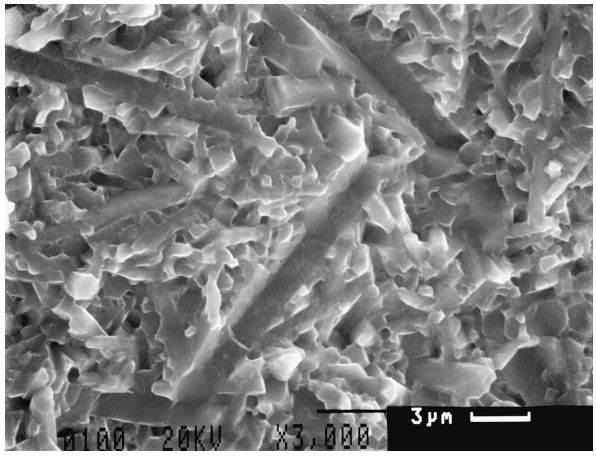

Fig. 2. The fracture surface of sintered SN-C silicon nitride ceramics.

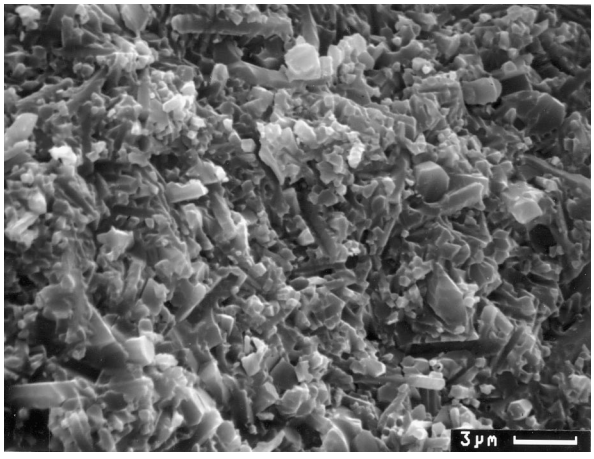

Fig. 1. Typical fracture surface of sintered SN-A and B silicon nitride ceramics.

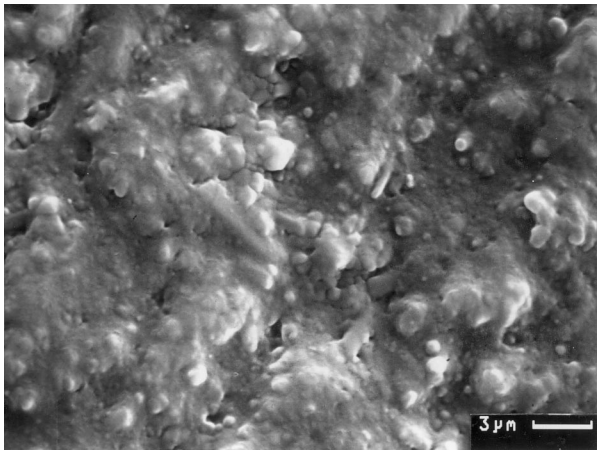

Fig. 3. The surface morphology of the SN-A silicon nitride ceramics.

on the free surface (Fig. 4). In addition, only a few populations of the subsurface pore clusters were found in the near surface region about 200 μm approaching toward the center from the surface for the SN-A ceramics; a significant contrast compared to previously reported results [5].

3.2. As-fired and machined bend strengths

Fig. 5. shows strength distributions of the differing silicon nitride samples with either the as-fired or machined surface subject to the bending tension. Their mean strengths and the corresponding Weibull moduli are summarized in Table 1. The as-fired strength as high as 750 MPa was obtained for the SN-A material which also presented the highest machined strength over 1 GPa in average. An interesting observation is that an enhanced "bulk" strength is seen to lead to an improved as-fired strength, suggesting that there may be some correlations between these two. In addition, the machined strengths show a Weibull modulus about twice that of the as-fired strengths, indicating that the failure of as-fired specimens is critically dependent on sintered surface conditions.

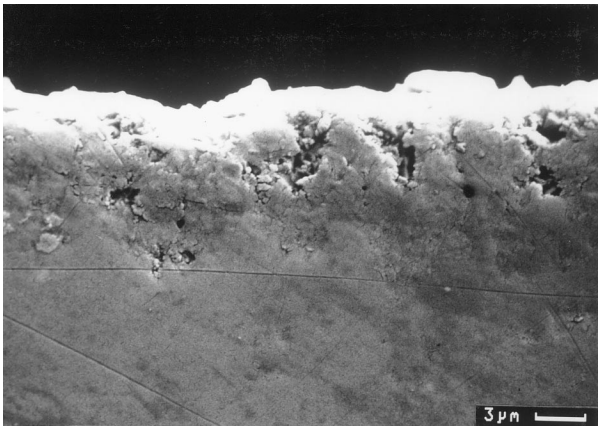

Fig. 4. Typical cross-sectional micrograph of the SN-A silicon nitride ceramics.

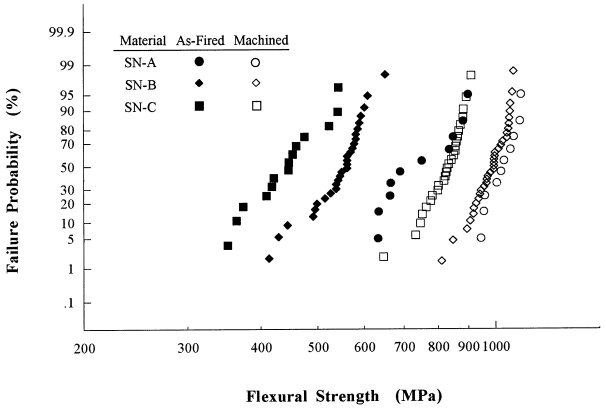

Fig. 5. Flexural strength distribution of the as-fired and machined, bulk samples.

Even though the fabrication process for the SN-A is unknown, it appears that the reduction of both surface and subsurface flaws is the main cause for the increased as-fired strength. This finding lies in the following observations. The smooth surface observed from the SN-A material would inherently minimize the severity of potential, unstable crack growth initiating from existing surface defects as the material is under tension. Comparing the strengths of SN-A and B, we could find that the "bulk" properties are almost indistinguishable (i.e. the difference between their machined strengths within their standard deviations), but the as-fired strength substantially differs by over 200 MPa. Therefore, the surface effect, especially crack-initiating defects located on the surface, is believed to be the most critical factor in determining the as-fired strength. This argument may be better illustrated from the findings that the comparatively smooth surface observed from the SN-A material would give rise to crack bluntings (of surface defects) as the materials are loaded under tension and hence an enhanced stress is necessary to initiate surface cracks, leading to an increase in the as-fired strength. If this happens, the nearest subsurface defects immediately adjacent to the surface (but not connected to the free surface) would then become prone to the unstable crack growth. This suggests that the surface defect alone is not the only variable influencing the as-fired strength. Table 1 vindicated that the material which presents a decreased bulk strength (i.e. the SN-C) also showed a reduced as-fired strength. This concurrent reduction in strength may have resulted from the observed microstructure found in the grain size difference (Figs. 1 and 2), since the abnormally grown β-Si_3N_4 grains were also found near the surface and might become fracture origins as stress exceeds a certain critical level, resulting in a total failure according to the weakest link theory. It hence, indicates that the subsurface defects (e.g. pores and large Si_3N_4 grains beneath the surface) are also critical to the as-fired properties. Therefore, the fracture of ceramics having an as-fired surface under tension could be deemed as a competing process of defect populations either located on or near the surface, subjected to an applied stress field where catastrophic failure would occur from either one depending on which fails first. Hence, the relative susceptibility of the surface and subsurface flaws to the applied stress would determine the magnitude of as-fired strength, consistent with the previous suggestion that the as-fired and machined strengths might be related.

3.3. The fracture model

A fracture analysis for modeling the relative significance of surface and subsurface flaws to the flexural

Table 1
Mean stress to failure and the corresponding Weibull modulus for the silicon nitride ceramics tested

Sample	Mean flexural strength (MPa)		Weibull modulus	
	As-fired[a]	Machined[a]	As-fired	Machined
SN-A	750 ± 106 (10)	1025 ± 59 (10)	8.2	20.1
SN-B	546 ± 55 (28)	982 ± 64 (33)	11.2	18.2
SN-C	445 ± 62 (14)	821 ± 59 (26)	8.4	18.2

[a] Number of specimens is given in parentheses.

strength of sintered ceramics has been conducted by assuming that defects are randomly dispersed in the material and the material is loaded under bending stresses. Considering some defects having a length a_1 intersecting the surface as shown in Fig. 6. (note that $h/2$ in the figure is the half-thickness of the bend bar), and some defects with a length $2a_2$ are dispersed at a distance b_1 below the surface. In the case where the flexural strength is controlled by the surface flaws, such as the surface defect with length a_1, the bend strength is given by [8].

$$\sigma_{f1} = \frac{K_{IC}}{\sqrt{\pi a_1}\, Y_1} \tag{1}$$

where σ_{f1} is the flexural strength determined by surface flaw with a crack length a_1, K_{IC} is the intrinsic fracture toughness of ceramics and Y_1 is the dimensionless parameter depending on the geometry of the specimen and the crack. In the case when $a_1/h < 0.1$ (i.e. for bend-bar thickness $h = 3$ mm, the upper bound of a_1 is hence smaller than 300 μm) Y_1 is then at a range of $1.042 < Y_1 < 1.122$.

Similarly, for the case where subsurface defects with a half- length a_2 determine the strength, the flexural strength can be expressed as (cf. the Appendix for detailed derivations)

$$\sigma_{f2} = \frac{K_{IC}}{\sqrt{\pi a_2}\, Y_2 \left(1 - \frac{2b_1}{h}\right)} \tag{2}$$

where σ_{f2} is the flexural strength determined by subsurface flaw with a length $2a_2$ and Y_2 is the dimensionless parameter given in the Appendix. The relative strength ratio for failures originating from either the surface or subsurface flaws is hence given by combining Eqs. (1) and (2) such that

$$\frac{\sigma_{f1}}{\sigma_{f2}} = \sqrt{\xi}\,\frac{Y_2}{Y_1}\left(1 - \frac{2b_1}{h}\right) \tag{3}$$

where we have defined a parameter ξ as the relation between surface and subsurface crack lengths, i.e.

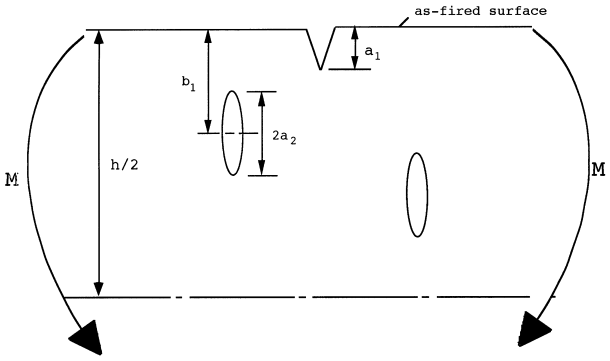

Fig. 6. Schematic of surface and bulk defects in silicon nitride bend bars under bending.

$$\xi = \frac{a_2}{a_1} \tag{4}$$

Examining Eq. (3) shows that the relative strength is determined primarily from, firstly, the relative length of the surface and subsurface defects and, secondly, the distance of the subsurface flaw to the free surface (note that for the case of subsurface flaws having the same size, it is the nearest flaw to the surface which fails). The length ratio ξ of cracks has a stronger influence on the strength ratio and the sample fails when the applied stresses exceed a certain critical value (i.e. either σ_{f1} or σ_{f2}, depending on which one is first reached).

For the case when $a_2/2b_1 < 0.5$ (crack "deep" below the surface), Eq. (3) can be approximately rewritten as

$$\frac{\sigma_{f1}}{\sigma_{f2}} = 0.97 \cdot \sqrt{\xi}\left(1 - \frac{2b_1}{h}\right) \tag{5}$$

Eq. (5) indicates that bulk defects located at a reasonably deep site under the free surface, control the strength if their length exceeds 2.3–2.8 times the length of surface flaws (for the case that b_1 ranges from 50 to 200 μm). Similarly, for the case when $0.8 < a_2/2b_1 < 0.9$ (crack "close" to the surface), Eq. (3) can be approximately rewritten as

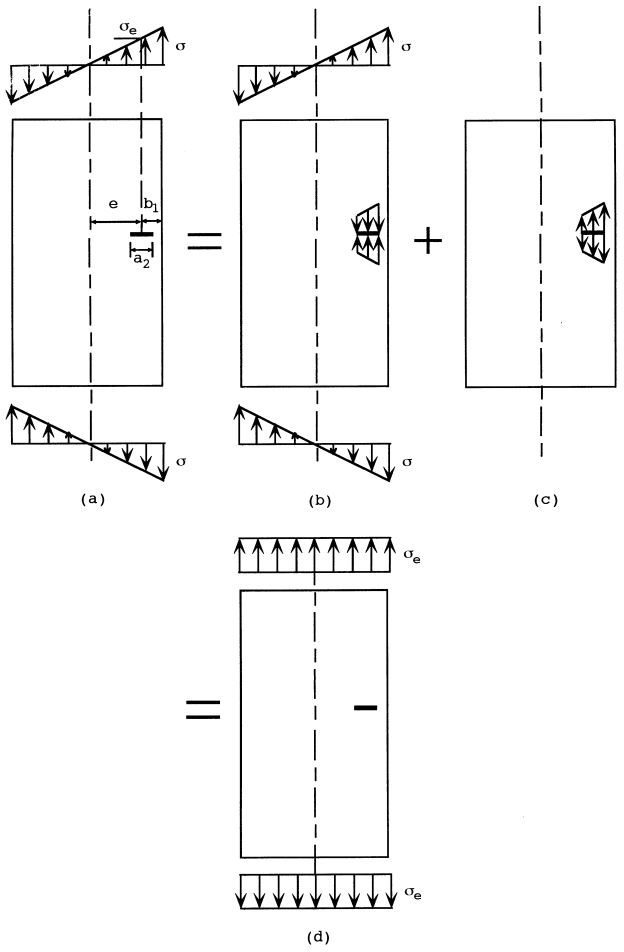

Fig. 7. Method of analysis for a bulk defect subjected to bending.

$$\frac{\sigma_{f1}}{\sigma_{f2}} = 1.45\cdot\sqrt{\xi}\left(1-\frac{2b_1}{h}\right) \tag{6}$$

In this case, even if the subsurface defect presenting a length identical to that of the surface defect (i.e. ξ equals to 1), the subsurface flaw becomes the dominate factor to the flexural strength.

Based on these derivations, we may conclude that bulk defects located at a reasonably deep site below the free surface control the as-fired strength if their length exceeds 2.3–2.8 times the length of the surface defects. The subsurface defect which is very close to the surface, however, is the most damaging and is not likely to be relieved by techniques such as surface coating since these defects are not connected to the surface and hence cannot be reached by the coating materials [7]. In such a case, a compressive residual stress would be beneficial to the as-fired strength [6,10]. Nevertheless, the derivation may be interpreted such that the as-fired strength would be solely dominated by surface conditions if bulk defects can be controlled within a given size range and distribution through, for example, an optimized powder processing. The as-fired strength would hence be expected to increase as the bulk strength increases (rather than by control of defect distribution, a reduction of the size of bulk defects is the most feasible approach in practice), agreeable with our experimental findings (Fig. 5). The modification of as-fired surface condition would become the next significant parameter for further enhancement of the surface strength.

4. Conclusions

The as-fired strength as high as 750 MPa was obtained for the sintered silicon nitride ceramics. Both the experimental results and theoretical derivations indicated that there are at least two conditions that must be met in order for an improved surface property on sintered ceramics. Firstly, the subsurface flaws have to be reduced to a significant size; otherwise, they may become the prominent strength-determining factor. In particular, near-surface defects must be eliminated through process optimizations. Secondly, surface defects with a reduced size and hence an increased "effective" crack length ratio ξ would then become beneficial to the as-fired properties. Combining these findings with the numerous methods published in the literature such as the surface coating [7] and an introduction of residual compression on surface [6,10] should provide a further strength enhancement for the as-fired surface strength of sintered ceramics.

Appendix

Considering the situation shown in Fig. 7, the stress intensity at the crack tip of the subsurface crack under the bending loading in Fig. 7(a) can be divided into a superposition of Fig. 7(b) and (c). Since Fig. 7(b) does not produce any stress intensity the stress condition of Fig. 7(a) is hence equivalent to that of Fig. 7(c). By further assuming that the crack length $2a_2$ is substantially smaller than the thickness of the bend bar, we may approximate the loading condition of Fig. 7(c) to that of Fig. 7(d), by replacing the bending tension to an "effective" tensile stress determined from the distance of the crack to the neutral axis as

$$\sigma_e = \sigma_{f2}\left(1-\frac{2b_1}{h}\right) \tag{A1}$$

where σ_e is the "effective" tensile stress. The stress condition of Fig. 7(a) is hence equivalent to that of Fig. 7(d) and the stress intensity solution for the crack tip near the free surface of Fig. 7(d) is given by [9]

$$K_{IC} = \sigma_e \sqrt{\pi a_2} Y_2 \quad \text{(A2)}$$

For the case where $2e/h$ [note that e is defined in Fig. 7(a) as the distance of the crack to the neutral axis) approaching toward 1, Y_2 varies as

$1.00 < Y_2 < 1.14$ for $a_2/b_1 < 0.5$ (defect "deep"

below the surface)

$1.14 < Y_2 < 1.40$ for $0.5 < a_2/b_1 < 0.8$

$1.40 < Y_2 < 1.72$ for $0.8 < a_2/b_1 < 0.9$ (defect "close"

to the surface).

References

[1] H. Kawamura, The construction and function in ceramic heat insulated engine, in: Ceramics, Powders, Corrosion and Advanced Processing Proceedings of Advanced Materials '93, I/A, Transactions of the Materials Research Society of Japan, Amsterdam, Netherlands, 1994, pp. 529–534.
[2] S.G. Winslow, Development of a cost-effective silicon nitride powder in DOE's ceramic technology project, Ceram. Eng. Sci. Proc. 14 (1–2) (1993) 360–369.
[3] G. Woetting, G. Leimer, H.A. Lindner, E. Gugel, Silicon nitride materials and components for industrial application, Ind. Ceram. 15 (1995) 191–196.
[4] N. Hirosaki, A. Okada, Effect of N_2 gas pressure sintering on the surface and strength of Si_3N_4, Adv. Ceram. Mater. 3 (1988) 515–516.
[5] W.J. Tseng, H. Kita, Determination of weak-surface-layer thickness of sintered Si_3N_4, Proceedings of Advanced Ceramics for Structural and Tribological Applications. Canadian Institute of Metals, Vancouver, Ottawa, 1995, pp. 589–598.
[6] W.J. Tseng, M. Taniguchi, T. Yamada, Transformation strengthening of as-fired zirconia ceramics. Ceram. Int. 25 (6) (1999) 545–550.
[7] H.-E. Kim, A.J. Moorhead, S.-H. Kim, Strengthening of alumina by formation of a mullite/glass layer on the surface, J. Am. Ceram. Soc. 80 (1997) 1877–1880.
[8] H. Tada, P. Paris, G. Irwin, The stress analysis of cracks handbook, Del Research Corporation, St. Louis, MO, 1973, pp. 2.13.
[9] H. Tada, P. Paris, G. Irwin, The stress analysis of cracks handbook, Del Research Corporation, St. Louis, MO, 1973, pp. 11.2.
[10] F.F. Lange, Compressive surface stresses developed in ceramics by an oxidation-induced phase change, J. Am. Ceram. Soc. 63 (1980) 38–40.